energies

MDPI

Article

Measurements Based Analysis of the Proton Exchange Membrane Fuel Cell Operation in Transient State and Power of Own Needs †

Andrzej Wilk * and Daniel Węcel

Department of Power Engineering and Turbomachinery, Silesian University of Technology, 18 Konarskiego st., 44-100 Gliwice, Poland; daniel.wecel@polsl.pl

* Correspondence: andrzej.t.wilk@polsl.pl; Tel.: +48-32-237-1115

† This paper is an extended version of conference proceedings: Wilk, A.; Węcel, D. Analysis of the Proton Exchange Membrane Fuel Cell in transient operation. *E3S Web Conf.* **2019**, *128*, 01026, also presented at the XII International Conference on Computational Heat, Mass and Momentum Transfer (ICCHMT2019), Rome, Italy, 3–6 September 2019.

Received: 30 November 2019; Accepted: 13 January 2020; Published: 20 January 2020

Abstract: Currently, fuel cells are increasingly used in industrial installations, means of transport, and household applications as a source of electricity and heat. The paper presents the results of experimental tests of a Proton Exchange Membrane Fuel Cell (PEMFC) at variable load, which characterizes the cell's operation in real installations. A detailed analysis of the power needed for operation fuel cell auxiliary devices (own needs power) was carried out. An analysis of net and gross efficiency was carried out in various operating conditions of the device. The measurements made show changes in the performance of the fuel cell during step changing or smooth changing of an electric load. Load was carried out as a change in the current or a change in the resistance of the receiver. The analysis covered the times of reaching steady states and the efficiency of the fuel cell system taking into account auxiliary devices. In the final part of the article, an analysis was made of the influence of the fuel cell duration of use on obtained parameters. The analysis of the measurement results will allow determination of the possibility of using fuel cells in installations with a rapidly changing load profile and indicate possible solutions to improve the performance of the installation.

Keywords: PEMFC; fuel cell; dynamic response; hydrogen; transient operation; own needs power

1. Introduction

Fuel cells are one of the technologies considered for the production of electricity and heat, which is supposed to allow for optimal use of fuels. These are devices in which there is a direct conversion of chemical energy of fuel into electricity, in electrochemical processes, without thermal and mechanical transformations. Therefore, they are not subject to restrictions of the Carnot cycle, thanks to which it is possible to achieve efficiency even above 60% at low temperatures [1]. Hydrogen fuel cells have undergone intensive development in recent years, from experimental solutions to fully commercial equipment [2]. The possibility of choosing different types of cells, with powers ranging from a few watts to even megawatts, allows using them in power supply systems of different kinds [3,4]. They can operate in individual power supply systems and can be connected to the power grid [5,6]. Hydrogen fuel cells do not have to work continuously, and they react quickly to load changes [7]. Unfortunately, a change in their parameters is observed during the work [8,9]. This is due to the relatively rapid degradation of the fuel cell components and their sensitivity to temperature.

Considering the possibility of using a Proton Exchange Membrane Fuel Cell (PEMFC) as the only power source in autonomous installations, one should consider their dynamic properties [10,11]. For

devices connected to the network, the dynamics of external devices should also be considered [12]. The tests carried out indicate rapid changes in the PEMFC voltage, exceeding the set state values, with step changes in the current [13]. The nature of changes in fuel cell voltage depends on the parameters, i.e., pressure or temperature, but first of all on the load power level and change in load current [14,15].

2. Test Facility

The applied power supply systems using fuel cells are built in the form of stacks consisting of several dozen to even several hundred individual fuel cells connected in series. Characteristics of fuel cells constructed in such a way do not depend significantly on the number of connected cells, i.e., on the power of the whole stack. They depend on the characteristics of a single cell. A low-power, water-cooled fuel cell was used in the research. Water cooling is typically used in higher power units where more efficient heat dissipation is required and at the same time it is easier to use the heat for heating purposes. Such solutions are used both in stationary and mobile systems (e.g., in transport). The results of the research will therefore be able to relate to fuel cells of higher power.

The fuel cell stack tested consists of 42 PEM cells connected in series, manufactured by Schunk Bahn-und Industrietechnik GmbH, type FC-42/HLC [16]. Its basic parameters are presented in Table 1.

The parameters achieved by the actual fuel cell may differ by up to 15% from the values stated by the manufacturer. This is due to the varying degrees of humidification of the membrane, its temperature, and the excess air ratio. The hydrogen consumption (with the required minimum purity of 99.99%) is 4 dm^3/min at rated load. To ensure continuity of substrate supply to the fuel cell, hydrogen is supplied with small overpressure (required to overcome flow losses). The air flow is forced by a compressor.

The fuel cell stack is connected to a control system equipped with a compressor (allowing to supply the regulated quantity of air to the cell, to ensure first of all a constant value of the excess air ratio), a hydrogen reducer (reducing the pressure of hydrogen taken from pressure vessels), a water cooling system (limiting the maximum working temperature of the cell), control and protection systems [17]. The system enables regulation of excess air ratio λ within 1.5 ÷ 4.0 every 0.1, cooling water temperature T_1 within 42 ÷ 56 °C every 1 °C. Figure 1 shows a diagram of the analyzed PEM fuel cell system with auxiliary devices.

Table 1. Test fuel cell parameters.

Parameter	Range
Operating voltage (V)	20 ÷ 45
Current (A)	max 18
Nominal power (W)	360
Excess air ratio	1.5 ÷ 4.0
Permitted inlet pressure range (bar)	1.0 ÷ 17.0
Hydrogen operating pressure (mbar)	50 ÷ 360
Hydrogen quality: Minimum	4.0 = 99.99%
Recommended	5.0 = 99.999%
Operating temperature (°C)	42 ÷ 55
Exhaust air temperature (°C)	10 ÷ 60
Ambient temperature (°C)	10 ÷ 30
Coolant temperature (°C)	10 ÷ 57
Heating power (W)	max 400
Maximum fuel consumption for rated output power (dm^3/min)	0 ÷ 4
Coolant volume flow rate (dm^3/h)	max 240
Coolant pressure (mbar)	max 320
Air volume flow rate (dm^3/min)	max 65
Air pressure (mbar)	max 400

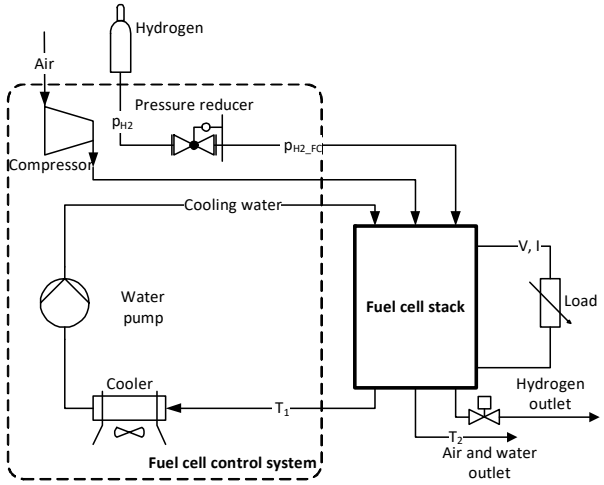

Figure 1. Diagram of the fuel cell stack measurement system.

The fuel cell control systems are generally programmed in a way to prevent damage of the fuel cell and at the same time to ensure the continuous operation of the system. For the tested fuel cell, the limits are maximum electric current (18 A), minimum voltage (20 V, corresponding to approximately the half of the non-load state), and maximum temperature of cooling water (57 °C). If these values are exceeded, the load of the fuel cell is disconnected within a short period of time. As a result of such conditions, the working area is very limited in comparison to the theoretical characteristics. The full characteristics of the tested FC-42/HLC fuel cell together with the working area are presented in Figure 2. It is possible to increase the electric current of the fuel cell up to 25 A and to reduce the voltage to 15 V only for a short period (about 1 s).

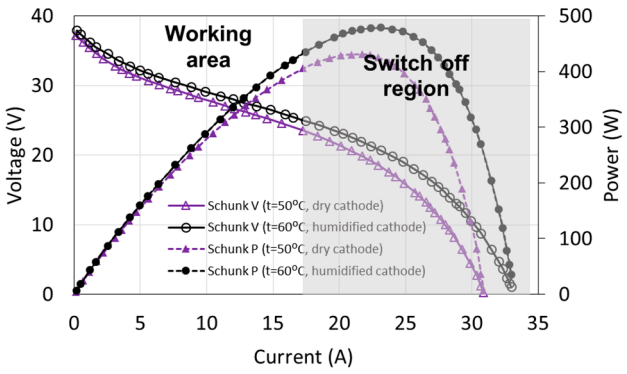

Figure 2. Fuel cell characteristics and operating area.

In order to improve the working conditions of the fuel cell, the control system opens the hydrogen outlet valve at certain intervals (depending on the load current), which results in the so-called purging of the fuel cell from the anode side. This allows the removal of excess moisture and the regeneration of the membrane, but at the same time the hydrogen flow is temporarily increased and the inlet pressure of p_{H2_FC} is reduced. The heat exchange in the cooling system is intensified by cyclically activated fans. This results in fluctuations in the operating temperature of the fuel cell. Therefore, it is difficult to maintain stable working conditions of a fuel cell. For this reason, the static characteristics obtained are approximate.

All auxiliary devices, i.e., compressor, cooling water pump, cooler fans, valves, measuring system were supplied from a separate source. The auxiliary power ΔP consumed by these units varied according to temperature of the cooling water and the load [18].

Some devices operate at constant power regardless of the fuel cell load. This applies to the circulating water pump and control and measuring system. Power consumed by the compressor and by the temperature control system depends on the load. Changes in compressor power occur together with changes in load results from the necessity to increase flow in order to maintain a constant ratio of excess air λ (Figure 3). An increase of λ significantly affects the value of ΔP, and linear relationships are obtained in the analyzed range of fuel cell current changes.

The frequency of opening of the anode purging valve also changes, which to a certain extent affects the consumed energy by the control system and, after averaging over time, the power of own needs. The opening time of the anode purging valve is approx. 0.4 s, and the frequency of opening the valve depends on the current of the fuel cell. The valve opens every 70 s in no-load steady state and every 55 s at nominal current [18]. Opening the valve increases the power ΔP by approx. 20 W.

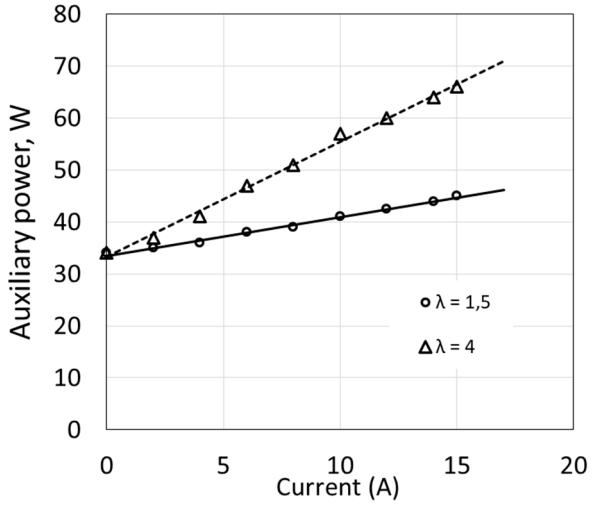

Figure 3. Power of fuel cell auxiliary devices as a function of electric current.

This does not result in a significant increase in the averaged over time value of the power of own needs, however, a significant increase in the demand for power of auxiliary equipment is temporarily achieved. In the case of direct supply of auxiliary devices from the fuel cell, the maximum current limit may be exceeded at the maximum load of the fuel cell. When the purge valve is opened, part of the hydrogen is released outside and does not participate in the process of electricity generation.

The last component of the auxiliary equipment is the fuel cell temperature control system, which consists of a cooling water pump, pipes supplying the coolant to the fuel cell, a radiator, and fans. The main element influencing the changes in the power of own needs are the fans. They are activated when the set cooling water temperature is exceeded and deactivated when the temperature drops below the set value. The power of the fans is approximately 13.5 W. The frequency of switching on depends on the set temperature and the load of the fuel cell.

The minimum and maximum values of the own power needs of the tested fuel cell are presented in Figure 4. Fuel cell operation with constantly running fans occurs only at high load and low set temperature, therefore the continuous line in Figure 4 representing Δ*P*max, Cooler ON is the limit value reached, when the fans run continuously. In practice, by averaging over time the used energy of own needs, usually lower powers of own needs than the limit value are obtained.

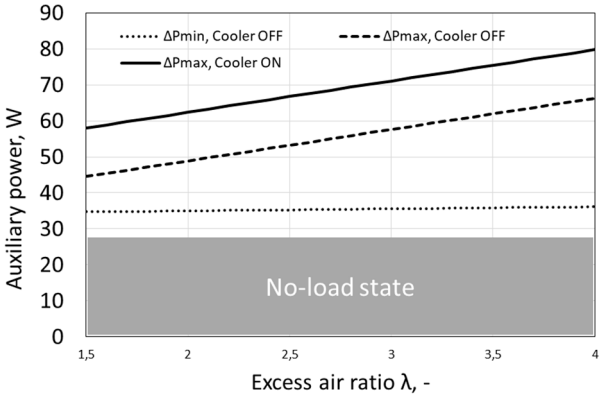

Figure 4. Power of fuel cell auxiliary devices as a function of excess air ratio.

The results obtained cannot be generalized to all fuel cell installations, but they reflect the trends and possible electricity demand of low power fuel cells. Taking into account the electric power generated by the fuel cell P, the auxiliary power index of such a device can be calculated (Equation (1)):

$$\delta_{FC} = \frac{\Delta P}{P}. \tag{1}$$

The dependence of the auxiliary power index δ_{FC} on the fuel cell current I at different air excess ratio λ is shown in Figure 5. Despite the increase in own needs power with increasing fuel cell load, the δ_{FC} indicator clearly decreases. The graph shows that the cell operation at a load below 10% of the rated power becomes pointless, because almost all the generated power is used to drive auxiliary devices.

The obtained auxiliary power index values are relatively high, because the auxiliary devices were designed for cooperation with a fuel cell with twice higher power. In the case of cooperation with such a fuel cell, the own needs index may even decrease below 10% [6].

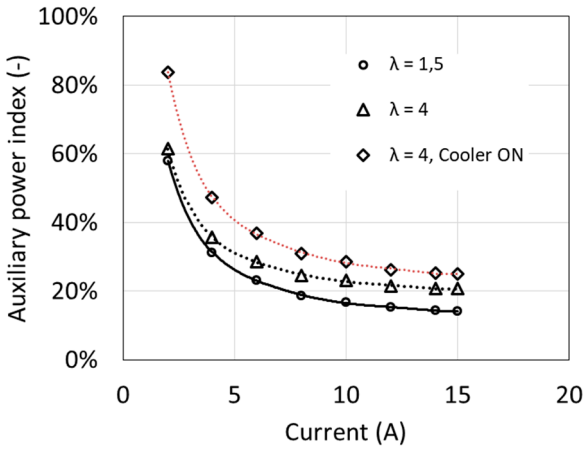

Figure 5. Fuel cell auxiliary power index as a function of current.

In the case of using a fuel cell as an autonomous source of electricity it is necessary to supply power to auxiliary devices. In most cases, this is done by using an additional battery pack. They provide power primarily during start-up and standby state of the fuel cell. During operation state, the fuel cell takes over the function of batteries, by using part of the electricity generated in the fuel cell stack for auxiliary devices supply, and at the same time recharges the batteries. Photovoltaic panels can also be used to supply power to auxiliary devices during fuel cell operation. If the fuel cell is connected to the power grid, the auxiliary devices can be constantly powered from the grid, so that the fuel cell can easily be turned off and restarted, and the auxiliary devices can be controlled regardless of the fuel cell's operation.

3. Static Characteristics of the Fuel Cell

The main operating characteristics allow determining the parameters of fuel cell operation for different loads and operating conditions. Examples of characteristics, determined for two temperatures and compared with the manufacturer's data, are shown in Figure 6.

Although the measurements were carried out on almost new cells (the total duration of use was several hours), the characteristics differed from those given by the manufacturer. The biggest differences can be observed in the maximum load area, where they even exceed 10%. This is characteristic for fuel cells with a significant degree of degradation [8,9].

The proper hydration of the polymer membrane, which acts as an electrolyte, has a very large impact on the correct and stable operation of the fuel cell, because its degree of hydration has a strict effect on the ionic conductivity of the electrolyte, needed to ensure the conductivity of protons. A quantity of water should be fed into the polymer membrane, which will keep the membrane humidity slightly below 100%, but at the same time remove its excess (in the form of water vapor), which is the result of the chemical reaction of combining hydrogen with oxygen at the cathode. Too much moisture causes condensation of water on the membrane and porous electrodes, contributing to blocking the flow path of air and hydrogen molecules, limiting the possibility of combining oxygen with the fuel. Usually it is not possible to directly control the moisture of the membrane and therefore other parameters are regulated that affect the fuel cell operation. Parameters that can be easily measured and set are air flow, air temperature, hydrogen humidity, and air humidity. A very simple way of adjusting the hydration of the membrane is to change the air flow. This is usually done by changing the flow rate of the compressor, which supplies air to the fuel cell. The air supplied also acts as an agent removing floating excess moisture, therefore too low an air flow results in excessive hydration of the membrane, while too high an air flow may cause excessive drying. Considering the above method of membrane hydration, different values of the excess air ratio λ should be set, which results in a change of air flow at a given load of the fuel cell. It is assumed that the humidity of the supply air does not change.

Adjusting the intake air temperature or the entire cell temperature is also a simple way to control the amount of moisture in the cell. The second method can only be implemented with the appropriate cooling system for the fuel cell stack e.g., by means of cooling water. Generally, hydration of the membrane is dependent on the operating temperature of the fuel cell, regardless of how this temperature is reached. A high temperature can lead to very fast drying of the membrane, while at low temperature moisture condensation from the air can occur, which also adversely affects the operation of the fuel cell. The gases flowing through the fuel cell react exothermically, which increases the temperature of the gas. Therefore, the set temperature of inlet gas to the fuel cell should be lower than the optimum operation temperature. The hydration of the polymer membrane methods described above should be considered together because they are related to each other. Optimal operating conditions of the fuel cell is obtained for the specific temperature, the excess air ratio, and air humidity [16]. Determining the relationship between the above quantities allows building a control system that will allow achieving high efficiency and high durability of fuel cells.

In this study, hydration of the polymer membrane was controlled indirectly by changing the excess air ratio and the operating temperatures of the fuel cell, which depends on the cooling system. Tests of the fuel cell in steady states enabled the determination of current and voltage characteristics for different operating temperatures T_1 (in the range $42 \div 54$ °C) and with different excess air ratio (in the range $\lambda = 1.5 \div 4$).

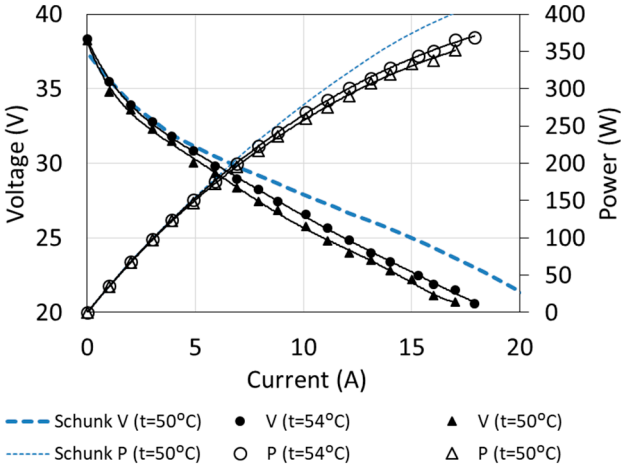

Figure 6. Fuel cell characteristics obtained by means of measurements.

The influence of both temperature T_1 and λ ratio on the characteristics of the cell was observed. The voltage, and thus the power of the fuel cell, increased by about 5% with the increase of the excess air ratio from the minimum to the maximum value (for the electric current of 14 A), as shown in Figure 7. At the same load (close to the rated load), the temperature increase by 1 °C caused the voltage to increase by about 0.7%. At low loads, the influence of temperature and λ ratio is much smaller [19–21].

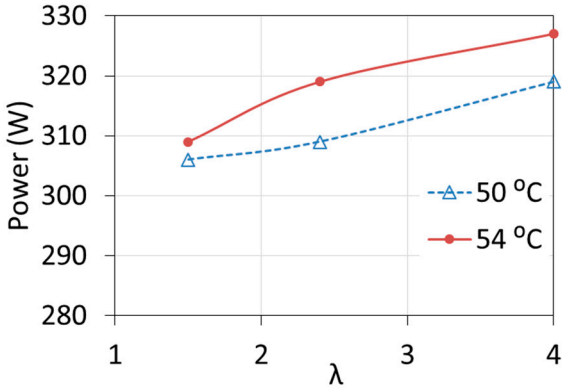

Figure 7. Changes in fuel cell power at different inlet coolant temperature T_1 and different excess air ratio λ.

The characteristics may also depend on the operation of a compressor supplying air that, at low electric currents and small values of the set excess air ratio λ, worked at minimum rotational speed without providing the set value of λ. In steady states, the flow rate of hydrogen q_{VH2} consumed was always directly proportional to the electric current I and it was independent of operating temperature and excess air ratio. The relationship between these quantities was determined on the basis of measurements and is described by Equation (2).

$$q_{VH2} = 5 \times 10^{-6} \cdot I \quad (2)$$

When determining the relationship in Equation (2), the volume of hydrogen used for purging the anode Δq_{VH2} was not taken into account, because all the characteristics of the fuel cell operation were determined for steady states. The anode purging process is cyclical therefore the Δq_{VH2} value should be taken into account only in the energy balance of the fuel cell system. The amount of hydrogen to purge the anode will primarily depend on the load and hydrogen operating pressure p_{H2_FC}. At maximum load, it is less than 5% of the total amount of hydrogen consumed.

The determined power characteristics (Figure 6) and the dependence on the hydrogen flow rate (Equation (2)) allow the calculation of fuel cell efficiency under various operating conditions. All calculations are made for steady-state cell operation and do not take into account time-averaged power for cyclical opening of the anode purging valve and starting of the radiator fans and hydrogen losses as a result of anode purging. Gross efficiency is calculated as the ratio of DC electric power produced by fuel cell to chemical energy contained in hydrogen that flow in 1 s into the fuel cell (Equation (3)). The hydrogen chemical energy was determined by using lower heating value of hydrogen (LHV_{H2} = 10.78 MJ/Nm^3).

$$\eta_g = \frac{P}{q_{VH2} \cdot LHV_{H2}}. \tag{3}$$

Figure 8 shows the gross efficiency of a fuel cell as a function of electric current for three values of the excess air ratio λ. The curves were determined for an operating temperature of 54 °C. Gross efficiency clearly decreases as the electric current increases, from 65% to less than 40% at maximum load. At the same time, in a fairly wide range of load (from minimum current up to about 12 A), it almost does not depend on the excess air factor λ. Only at higher loads, higher efficiency values are obtained at the higher value of the air excess ratio λ. A larger amount of supplied air allowed for higher electric currents and thus higher powers.

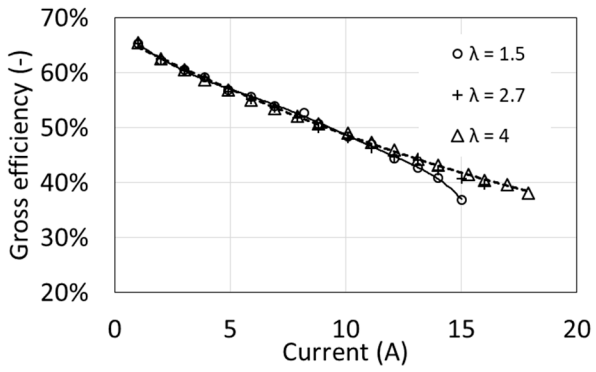

Figure 8. Characteristics of the gross efficiency as a function of excess air ratio λ for T_1 = 54 °C.

The net efficiency is calculated as the ratio of DC electric power generated by the fuel cell reduced by the power of auxiliary devices (power of own needs) to chemical energy contained in hydrogen that flows in 1 s into the fuel cell (Equation (4)).

$$\eta_n = \frac{P - \Delta P}{q_{VH2} \cdot LHV_{H2}}. \tag{4}$$

Due to the clearly different power demand of the auxiliary devices obtained at different values of the air excess ratio λ (Figure 3), the net efficiencies are also clearly different (Figure 9). Maximum efficiency is obtained at around half of the maximum power, reaching approx. 40% for λ = 4 and 44% for λ = 1.5. At maximum power, the net efficiency decreases to approximately 30%. These values are relatively low, but they result from high values of the auxiliary power index.

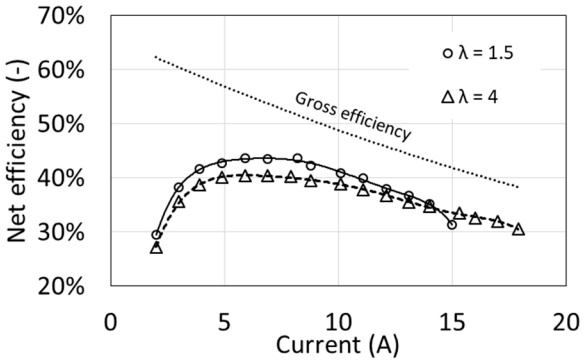

Figure 9. Characteristics of the net efficiency as a function of air excess ratio λ for T_1 = 54 °C.

From the point of view of efficiency, fuel cell operation at a smaller excess air ratio λ is more advantageous, provided that the load is lower than the maximum. However, for operational reasons, it seems fuel cell operation with a higher excess air ratio is better. Higher powers are available, and at maximum load the net efficiency is higher and its characteristics curve as a function of current are flatter. The net efficiency will decrease by several percentage points if the additional power of the radiator fans is taken into account, whose start-up depends on the fuel cell load and the set coolant temperature.

4. Transient Tests

When analyzing the operation of fuel cells, several states may be taken into account: start-up, no load, increase of load, operation under constant load, reduction of load, shutdown. The article focuses only on the work of the cell itself, and does not analyze the preparation for work and the transient states of auxiliary equipment. It is assumed that all these devices are ready for operation. During the start-up of PEMFC it is necessary to remove air from the anode pipes. This can be achieved with inert gas (e.g., nitrogen) and then hydrogen must be supplied to activate the anode. However, the moist air supply from the cathode side allows the membrane to be pre-humidified. These actions always take place without a load and are intended to achieve at least the rated voltage (for the tested cell 24 V). The start-up process can take from a few to several dozen seconds, depending on the size of the installation and the time that has elapsed since the last start-up, and can be completed when the voltage reaches a value close to non-load state [22]. For the fuel cell under analysis, the minimum starting time from cold start to rated output is about 2 min.

In the non-load state, the fuel cell is prepared to connect the load. On the anode side there is hydrogen with appropriate parameters and air is supplied to the cathode side. The membrane is moistened to allow proton conduction. The no-load condition is always present when the load is disconnected. The no-load voltage may vary depending on the degree of humidification of the membrane, the temperature, and the degree of degradation of the fuel cell. In this state, it is necessary to power the auxiliary equipment from a separate source. In fuel cells of high power, it is necessary to use compressors allowing for air supply to the cathode channels.

At a constant pressure of hydrogen supply from the pressure reservoir (2 bars), the reduction valve keeps the operating pressure p_{H2_FC} of the hydrogen at the inlet to the anode between 300 and 310 mbar. It depends on the current of the fuel cell. Lower pressure is achieved at maximum load. At the moment of anode purging the operating pressure drops can be observed to 280 mbar, but they do not have a significant influence on the voltage and current of the fuel cell. In all tests, the value of the excess air ratio was set to λ = 4.

Fuel cells are DC power sources therefore they are connected to resistive receivers. All tests were carried out with the use of electronic load, which allowed for a rapid change of resistance. This way of loading the fuel cell is closer to the real operating conditions. The main parameters analyzed in the tests were voltage and current of the cell, which determine the obtained power.

Indicators of Changes in Fuel Cell Parameters

In order to describe the transition states in the fuel cell, several indicators have been defined [23].

Voltage fluctuation rate ε_V—dimensionless value indicating the difference between the temporary value of voltage and the voltage in the steady state (Equation (5)).

$$\varepsilon_V = \frac{|V_i - V_s|}{V_s}. \tag{5}$$

Maximum voltage deviation from the steady value ΔV_{max}—a value indicating the maximum difference between the temporary value of voltage after load change and the voltage in the steady state (Equation (6)).

$$\Delta V_{max} = \left|V_{i(min/max)} - V_s\right|. \tag{6}$$

Voltage response time τ_V—time from load change to voltage fluctuation rate below 2% (Equation (7)).

$$\tau_V = t(\varepsilon_V \leq 2\%) \tag{7}$$

5. Results and Discussion

5.1. Changing the Load of the Fuel Cell

The fuel cell was started (after two weeks of downtime) and loaded to moisten the membrane and stabilize the operating conditions. It took about 20 min to prepare the fuel cell for research. The tests began with the connection of a receiver with a constant resistance. Figure 10 shows changes in fuel cell parameters when the electrical circuit is connected with a resistance of 3 Ω. It corresponds to a load of approx. 60% of the rated value. The circuit was opened after 600 s and reloaded with the same resistance after next 120 s.

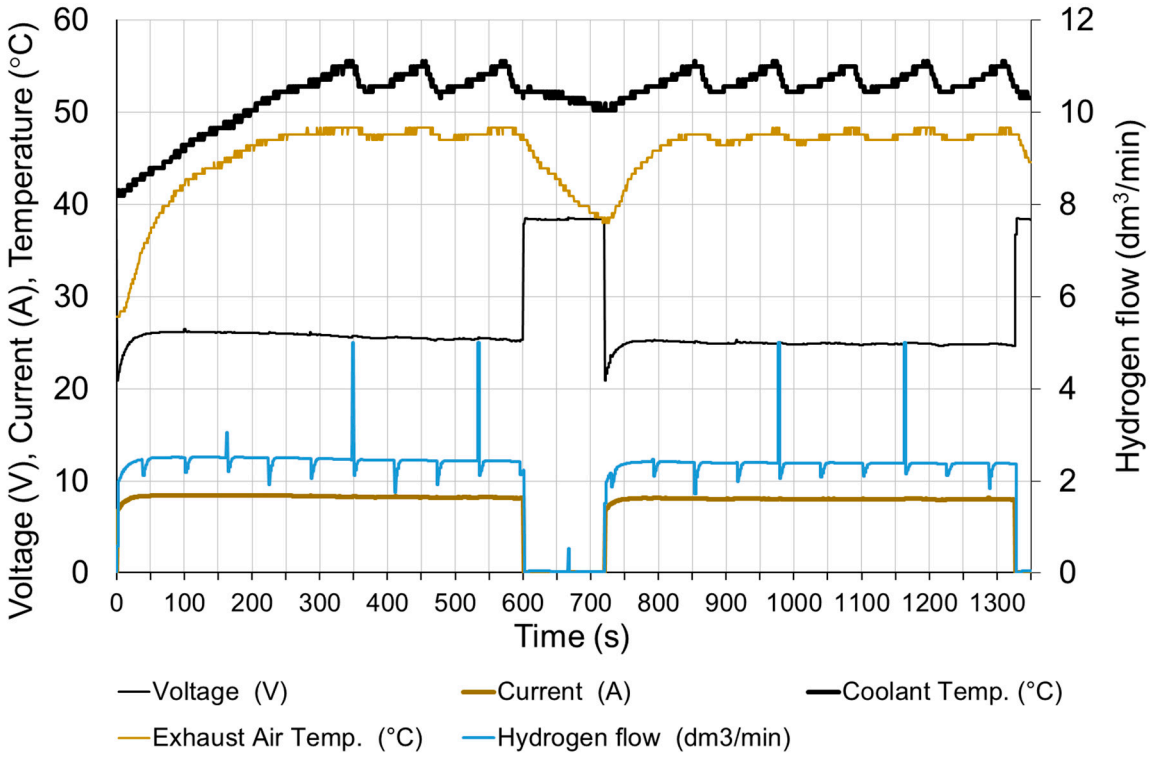

Figure 10. Fuel cell parameters changes at rapid increase of load.

Before the load, the cell operated for about 15 min with the resistance of the receiver 1.5 Ω, therefore, before the first series of measurements, the cell was heated, and the cooling water had the temperature at the inlet T_0 = 32 °C.

At the moment of a rapid load (in less than 0.1 s), the current increases to approx. 80% of the steady state and within 30 s reaches 98% of the steady state. The voltage drops rapidly below the steady state value and then rises to 98% of the steady state value after 30 s. It is assumed that the steady state is reached when the exhaust air temperature T_2 is stable. The time to reach steady state depends on the initial temperature of the fuel cell. The parameters of fuel cell are stable except voltage—slow decreasing of voltage within 20 min after the load is switched on can be observed.

In addition to electricity generation, the fuel cell is also a source of heat. The amount of heat produced is dependent on the current [24]. In the case of water-cooled fuel cells, most of the heat is transferred to the cooling system. Only a small part of the generated heat is discharged together with the exhaust air (approximately 5 %) and via the housing into the environment [18]. The cooling water flow is constant, so increasing the load of the fuel cell increases the operating temperature. Due to temperature restrictions, the temperature of the cooling water does not exceed 57 °C. This is due to the periodical operation of the radiator fans. The starting moment of the fans is clearly visible in Figure 10, when the temperature of the cooling medium starts to drop rapidly with the unchanged load. This method of cooling stabilizes the temperature and its fluctuations are 2 ÷ 5 °C.

The hydrogen flow is proportional to the current. The visible momentary fluctuation of the stream is due to the purging of the anode. With a constant current of the fuel cell, the purge valve opens at equal intervals. The hydrogen flow temporarily increases to its maximum value and then decreases due to the necessity to increase the operating pressure in the anode area. Purging the anode causes a slight increase in the voltage of the cell by about 0.5%. The voltage returns to the previous value after approx. 10 s. The time characteristics shown in Figure 11 were obtained, when the load was switched on again, therefore the time scale starts from 720 s. In the long period, anode purging has a positive effect on the stabilization of the fuel cell operating conditions.

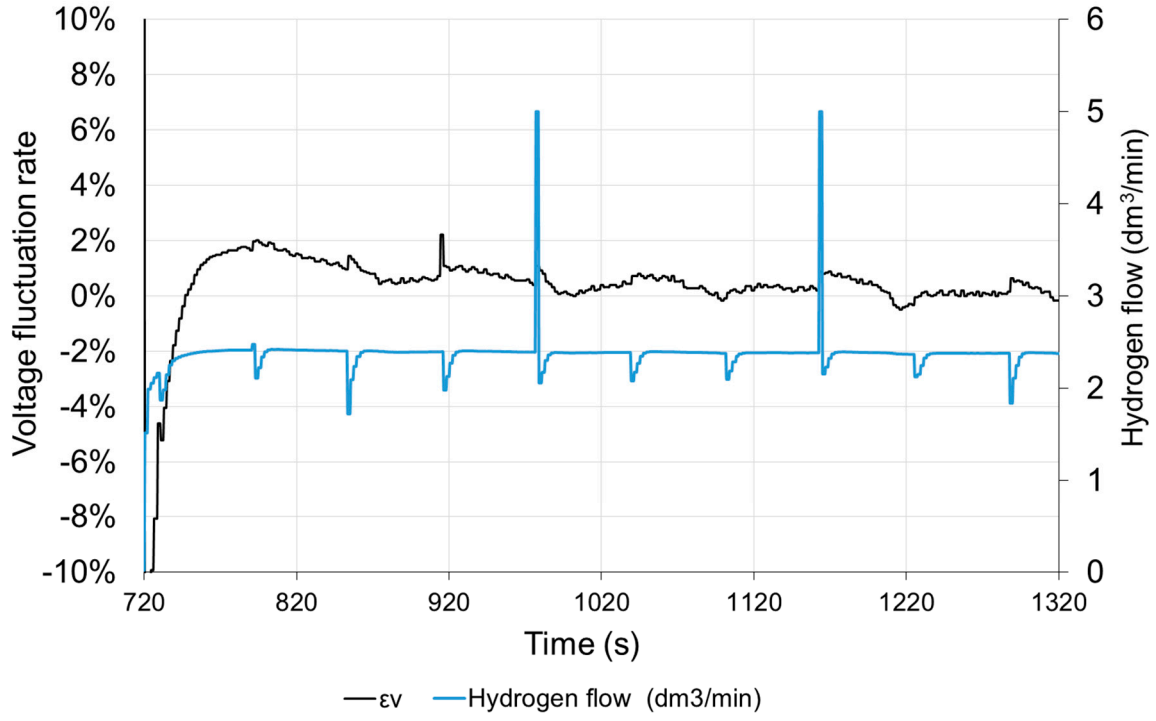

Figure 11. Voltage fluctuation rate ε_V and hydrogen flow with time under step resistance change.

5.2. Step Increase and Decrease of Fuel Cell Load

Subsequent tests were carried out by increasing and then decreasing in steps the resistance of the receiver. Such a method of load of the power source corresponds in practice to connecting successive receivers [25]. The operating time at subsequent loads was 5 min.

In Figures 12 and 13 it can be seen that the greatest deviation of voltage from the stable value occurs at the transition from non-load to low load and when the load is reduced to small values. With these changes, the time of setting the voltage τ_V to the level of 98% of the set value is approx. 50 s. Load changes while the cell is in operation do not cause significant voltage changes. The fixed value is reached in less than 1 s. When the load increases (the resistance of the receiver decreases), the voltage drops rapidly below the set value and then increases (this is particularly visible for low load—Figure 14). When increasing the load, the voltage on the fuel cell increases rapidly above the set value, and then decreases to the voltage of the set state (Figure 15). The lines on Figures 14 and 15 show voltage changes obtained at a step change of the load described by the value of the current in steady states. In all analyzed cases the resistance of the receiver was changed, so that the nature of the changes in the current is the same as the voltage.

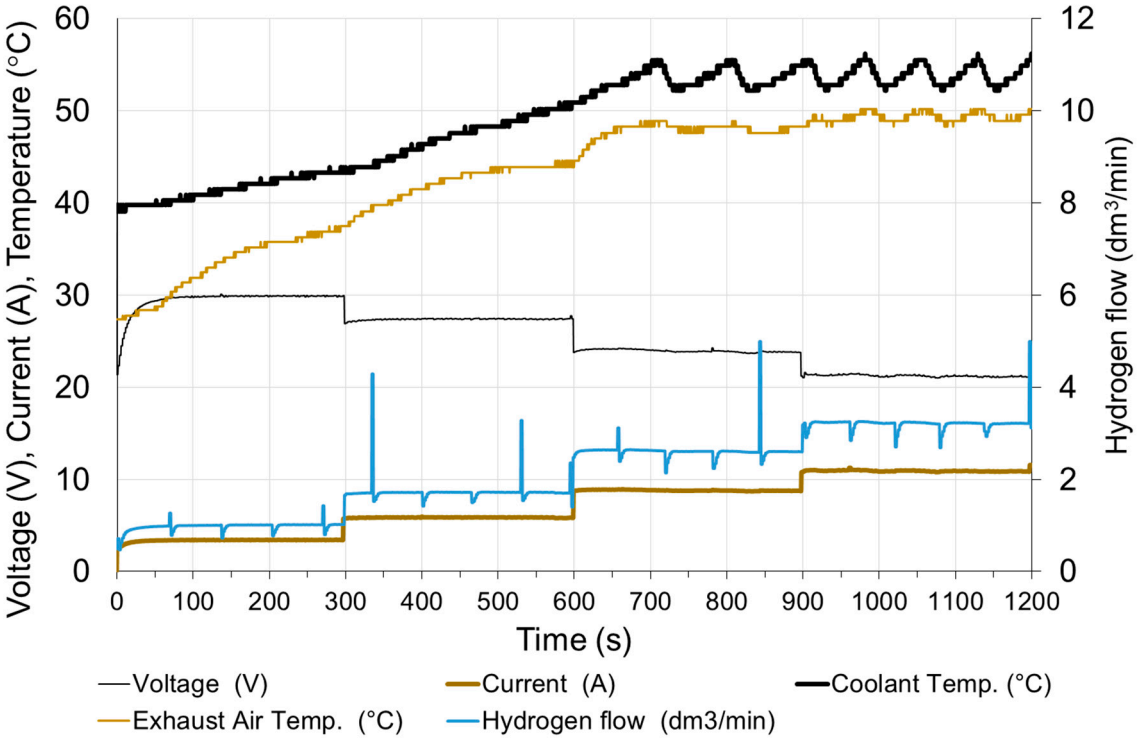

Figure 12. Changes in fuel cell parameters during step increasing of the load.

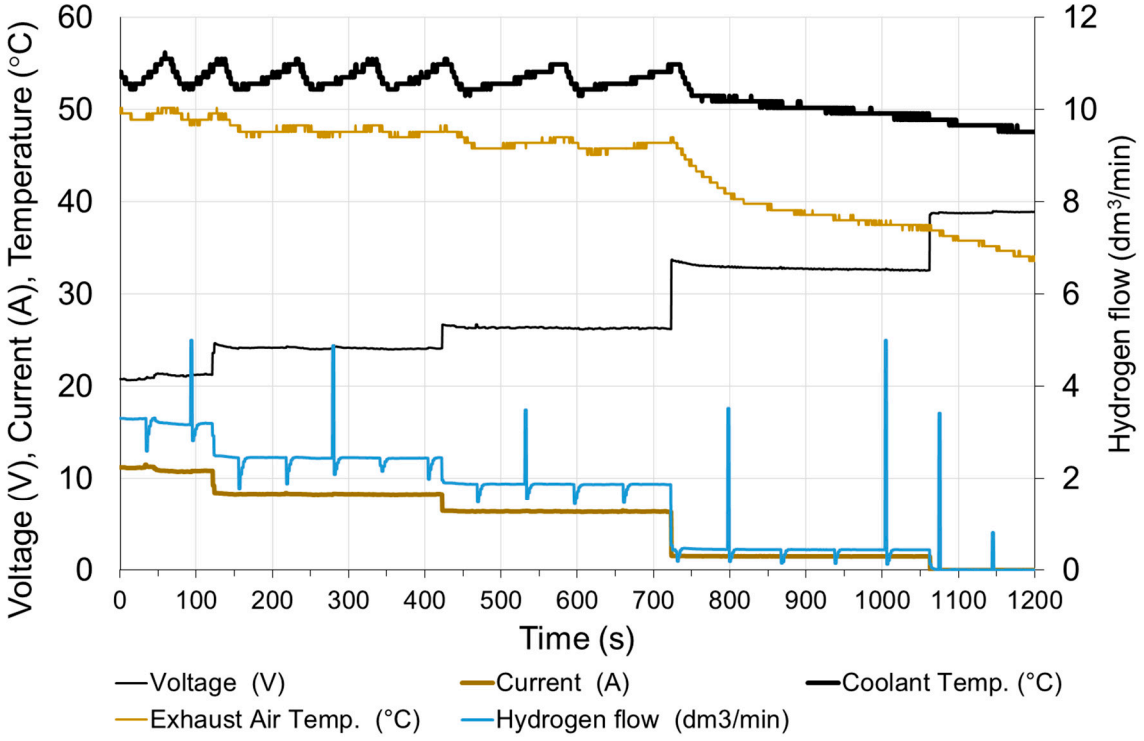

Figure 13. Changes in fuel cell parameters during step decreasing of the load.

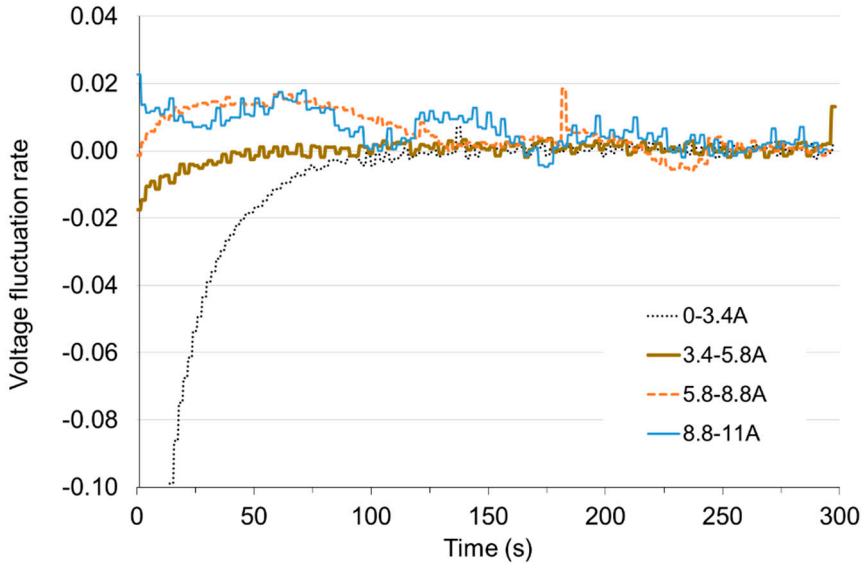

Figure 14. Voltage fluctuation rate ε_V with time under load increase.

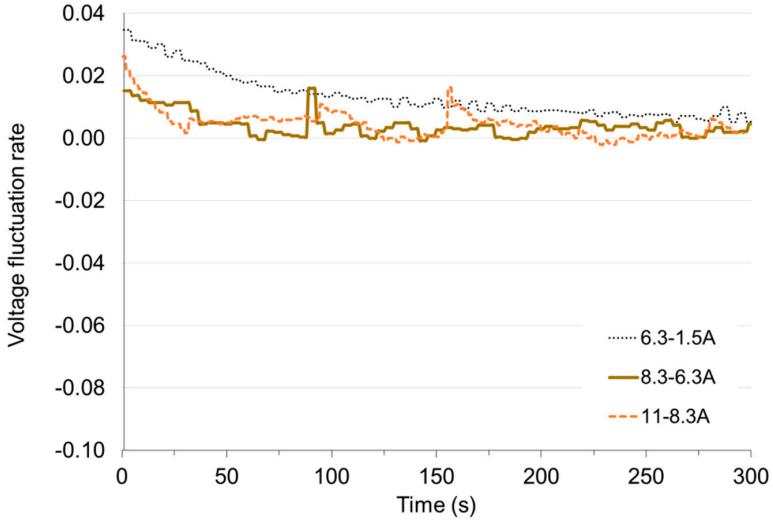

Figure 15. Voltage fluctuation rate ε_V with time under load decrease.

In the case of DC sources, the power generated is a square function of the current. The power generated by the fuel cell thus changes in the same way as the current, and only the fluctuations are more significant.

At high loads, although the voltage very quickly reaches the set state, the fluctuations resulting from anode purging and higher temperature fluctuations are visible clearly. This is due to the fact that at higher loads the heat flow generated in the fuel cell increases, which results in an increase of the frequency of switching on the fans in the cooling system.

Delay in reaching the appropriate electric power after a step change in load (decrease or increase of resistance), e.g., by turning the receivers on or off, may result in their incorrect operation. In practice fuel cells are connected to batteries or supercapacitors via a DC/DC converter, in order to eliminate these phenomena [11]. Additional power sources support the operation of the fuel cell in transient states, i.e., provide power if the load increases and get power while reducing the load. Simultaneously, they are used to supply power to the auxiliary devices, without which the fuel cell would not be able to work.

6. Fuel Cell Durability

One of the basic disadvantages of hydrogen fuel cells is their low durability [26]. The wear and tear of cell components is so-called anode poisoning [27]. In most cases, due to the fuel cell wear and tear, deterioration of voltage-current characteristics and a decrease of voltage in no-load state occur [28,29]. It also causes a decrease of fuel cell efficiency [30].

For the tested PEM fuel cell, the manufacturer specified the service life over 1500 h. This is the time after which the output power is at least 90% of the nominal power. The condition for achieving such durability is the fuel cell operation in conditions not exceeding the imposed restrictions. Factors shortening the above service time are work at excess temperature, undervoltage, hydrogen depletion, and hydrogen or air contamination.

Due to the relatively short duration of use of the tested fuel cell, the results of testing another fuel cell were used to determine the impact of operating time on operating parameters. It was the same type of cell but with two times higher power (720 W), which was used for almost 10 years. The producer defined its service life as over 500 h [17].

Due to operation of the fuel cell in different conditions and with different loads (also in non-load state), the actual working time was not recorded.

The first start-up took place in October 2009. Then the fuel cell was used quite intensively until the end of 2010 during cycles of research. Over next years, the fuel cell has been operated several

times a year. Usually, at each start-up, tests were carried out to determine the characteristics of the fuel cell at different operating parameters. The full range of tests was not always carried out, so the characteristics for each excess air ratio λ and for each fuel cell temperature T_1 were not obtained every year. The voltage-current characteristics and obtained power in different years of fuel cell operation are shown in Figures 16 and 17. The graphs also show the nominal characteristics of a fuel cell provided by the manufacturer for λ = 3 and T_1 = 65 °C.

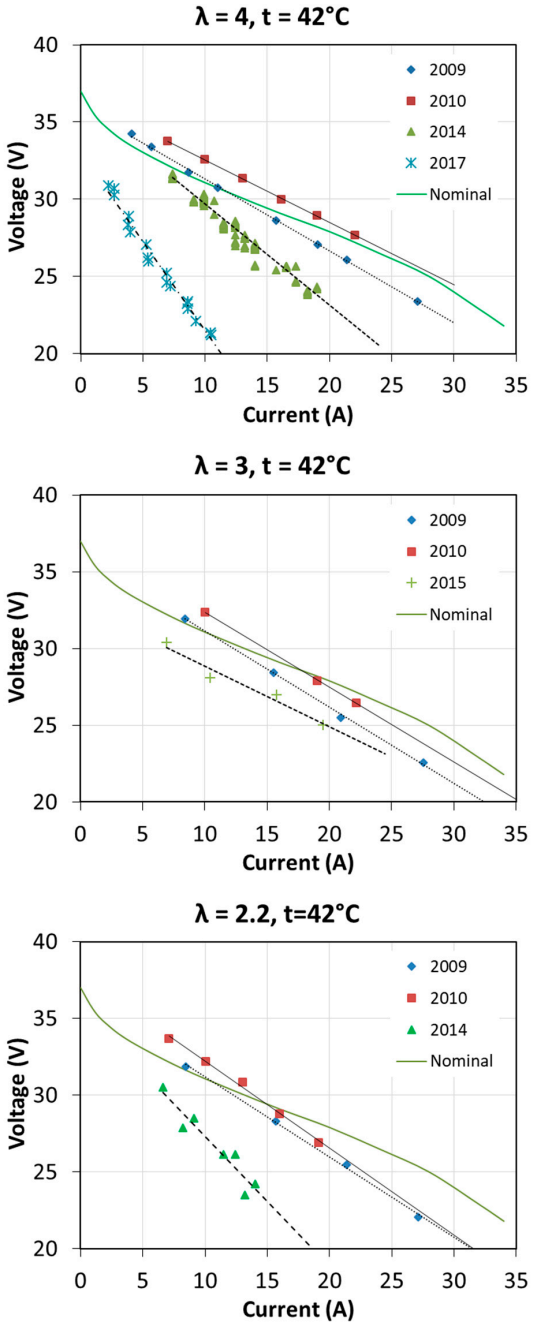

Figure 16. Fuel cell characteristics V = f(I) obtained during many years of operation.

The characteristics presented in Figure 16 differ from the manufacturer's data, which results mainly from other operating parameters, i.e., fuel cell temperature. The test station allowed obtaining the maximum temperature of 54 °C. It is interesting to note that after a year of intensive operation, an increase of V = f(I) by a few volts was obtained, practically for all operating conditions. Fuel cell performance parameters in some areas exceeded the nominal parameters. This was due to the proper

moistening of the membrane and proper operation. Open-circuit voltage according to the manufacturer should be 37 V, while at the beginning of operation this voltage was even above 40 V. In the subsequent years, a visible degradation of the fuel cell was observed, which is related to obtaining increasingly lower voltages during the load of the fuel cell with the same current. After 8 years of operation, the achievable current was even twice as low as at the initial state.

In the case of power characteristics P = f (I) it can also be seen that in the first year of operation, the obtained electric power was higher, even by 10% above the nominal value. In the subsequent years of fuel cell operation, the power characteristics were significantly decreased. The maximum electric powers, for the presented operating conditions after 7 years of operation, did not exceed 35% of the nominal power. In each of the analyzed cases, larger differences in the obtained characteristics occur at higher electric currents.

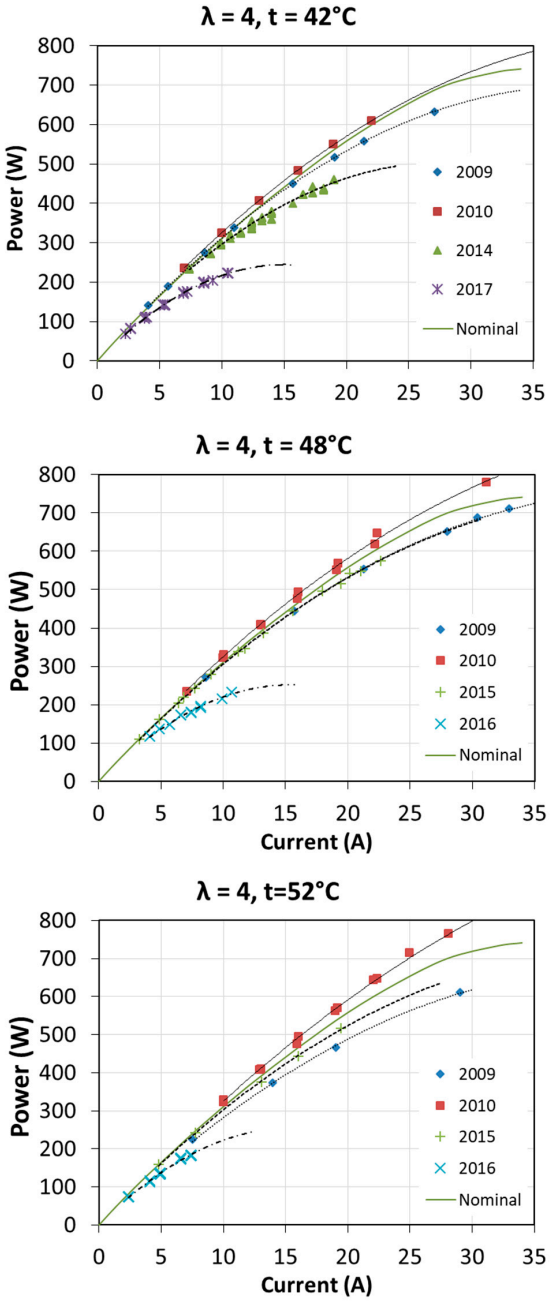

Figure 17. Fuel cell characteristics P = f(I) obtained during many years of operation.

7. Conclusions

The main purpose of the research was to check how the parameters of a fuel cell change when the resistance of the receiver changes and whether it is possible to provide adequate power of the fuel cell to power the receivers in a short time. Another part of the research was to determine the fuel cell efficiency depending on the load, taking into account also fuel cell auxiliary power. The last part of paper describes durability analysis of a PEM fuel cell.

The test shows that PEMFC reacts very quickly to changes in load, but moves relatively slowly to a steady state at a steep increase in load from non-load state. When only a load change occurs, the duration of the voltage response time τ_V of the fuel cell is several seconds. At low currents this time can be extended up to 50 s. Small voltage changes can be observed even up to 300 s after a jumping load change occurs. This is related to the determination of the temperature of the fuel cell and the anode purging process.

During a load change, the PEMFC operating point did not move along the steady state line, which can cause the limit values to be exceeded under adverse conditions and when the load increases too much. This applies mainly to the limitation of the minimum voltage value. The consequence of this may be the switching off of the fuel cell, even though the fuel cell in the steady state should work at a given load.

Taking into account the amount of electricity produced and the amount of hydrogen consumed during the dynamic change of load tests, the efficiency of the fuel cell tested is approximately 43%. This value can be considered to be relatively high, especially when considering the operation of a cell with frequent changes of load. The calculation of efficiency does not take into account the energy of internal loads. Efficiency in steady state depends heavily on the load and operation parameters of the fuel cell. If auxiliary power is taken into account, the fuel cell efficiency decreases by several percent. From the fuel cell operation point of view, durability is more important than efficiency, because it significantly affects the achieved power, as the test results show.

Author Contributions: Conceptualization, A.W. and D.W.; Methodology, A.W. and D.W.; Software, A.W. and D.W.; Validation, A.W. and D.W.; Formal Analysis, A.W. and D.W.; Investigation, A.W. and D.W.; Resources, A.W. and D.W.; Data Curation, A.W. and D.W.; Writing-Original Draft Preparation, A.W. and D.W.; Writing-Review & Editing, A.W. and D.W.; Visualization, A.W. and D.W.; Supervision, A.W. All authors have read and agreed to the published version of the manuscript.

Funding: This research was funded by Rector of Silesian University of Technology grant number RGJ no 08/050/RGJ18/0152.

Acknowledgments: This publication was supported as a part of the Rector's grant in the area of scientific research and development works, Silesian University of Technology, Poland, grant number RGJ no 08/050/RGJ18/0152.

Conflicts of Interest: The authors declare no conflict of interest.

Nomenclature

V	operating voltage (V)
V_i	transient voltage (V)
I	fuel cell current (A)
V_s	steady-state voltage (V)
T_0	inlet coolant temperature (°C)
T_1	outlet coolant temperature (°C)
T_2	exhaust air temperature (°C)
p_{H2}	hydrogen inlet pressure (bar)
p_{H2_FC}	hydrogen operating pressure (mbar)
q_{VH2}	hydrogen flow rate (Nm^3/s)
t	time (s)
τ_V	voltage response time (s)
P	power (W)

ΔP	power of auxiliary devices (W)
ΔV_{max}	maximum voltage deviation (V)
Δq_{VH2}	volume of hydrogen for anode purging (Nm^3/s)
δ_{FC}	auxiliary power index (-)
λ	excess air ratio (-)
η_g	gross efficiency (-)
η_n	net efficiency (-)

References

1. Larminie, J.; Dicks, A. *Fuel Cell Systems Explained*, 2nd ed.; John Wiley Sons Ltd.: Chichester, UK, 2003; ISBN 0-470-84857-X.
2. Bartela, Ł.; Kotowicz, J.; Dubiel, K. Technical—Economic comparative analysis of energy storage systems equipped with a hydrogen generation installation. *J. Power Technol.* **2016**, *96*, 92–100.
3. Barelli, L.; Bidini, G.; Gallorini, F.; Ottaviano, A. Dynamic analysis of PEMFC-based CHP systems for domestic application. *Appl. Energy* **2012**, *91*, 13–28. [CrossRef]
4. E4tech, The Fuel Cell Industry Review 2018. Available online: https//:www.califirniahydrogen.org/wp-content/uploads/2019/01/TheFuelCellIndustryReview2018.pdf (accessed on 20 July 2019).
5. Wang, Y.; Chen, K.S.; Mishler, J. A review of polymer electrolyte membrane fuel cells: Technology, applications, and needs on fundamental research. *Appl. Energy* **2011**, *88*, 981–1007. [CrossRef]
6. Kotowicz, J.; Węcel, D.; Jurczyk, M. Analysis of component operation in power-to-gas-to-power installations. *Appl. Energy* **2018**, *216*, 45–59. [CrossRef]
7. Tang, Y.; Yuan, W.; Pan, M. Experimental investigation on the dynamic performance of a hybrid PEM fuel cell/battery system for lightweight electric vehicle application. *Appl. Energy* **2011**, *88*, 68–76. [CrossRef]
8. Aquino, A.; Heng, J. *Current and Temperature Distributions in a PEM Fuel Cell, A Major Qualifying Project Report Submitted to the Faculty of Worcester Polytechnic Institute*; Worcester Polytechnic Institute: Worcester, MA, USA, 2017.
9. Verhage, A.J.L.; Coolegem, J.F.; Mulder, M.J.J.; Yildirim, M.H.; de Bruijn, F.A. 30,000 h operation of a 70 kW stationary PEM fuel cell system using hydrogen from a chlorine factory. *Int. J. Hydrogen Energy* **2013**, *38*, 4714–4724. [CrossRef]
10. Cieśliński, J.T.; Kaczmarczyk, T.Z.; Dawidowicz, B. Dynamic characteristics of the proton exchange membrane fuel cell module. *Arch. Thermodyn.* **2018**, *39*, 125–140.
11. Do, T.; Truong, H.; Dao, H.; Ho, C.; To, X.; Dang, T.; Ahn, K. Energy Management Strategy of a PEM Fuel Cell Excavator with a Supercapacitor/Battery Hybrid Power Source. *Energies* **2019**, *12*, 4362. [CrossRef]
12. Witkowski, A.; Rusin, A.; Majkut, M.; Stolecka, K. Comprehensive analysis of hydrogen compression and pipeline transportation from thermodynamics and safety aspects. *Energy* **2017**, *141*, 2508–2518. [CrossRef]
13. Hamelin, J.; Agbossou, K.; Laperriere, A. Dynamic behavior of a PEM fuel cell stack for stationary applications. *Int. J. Hydrogen Energy* **2001**, *26*, 625–629. [CrossRef]
14. Sun, H.; Zhang, G.; Guo, L. A Study of dynamic characteristics of PEM fuel cells by measuring local currents. *Int. J. Hydrogen Energy* **2009**, *34*, 5529–5536. [CrossRef]
15. Cho, J.; Kim, H.S.; Min, K. Transient response of a unit proton-exchange membrane fuel cell under various operating conditions. *J. Power Sources* **2008**, *185*, 118–128. [CrossRef]
16. *Handbuch für Schunk Brennstoffzellen-Stacks FC-42/HLC*; Schunk Bahn-und Industrietechnik GmbH: Wettenberg, Germany, 2010.
17. *FC-42 Evaluation Kit, Instruction Manual*; Version 1; Heliocentris Energiesysteme GmbH: Berlin, Germany, 2009.
18. Ogulewicz, W.; Węcel, D.; Wiciak, G.; Łukowicz, H.; Kotowicz, J.; Chmielniak, T. *Pozyskiwanie energii z ogniw paliwowych typu PEM chłodzonych cieczą*; Monografia, Wydawnictwo Politechniki Śląskiej: Gliwice, Poland, 2010.
19. San Martín, I.; Ursúa, A.; Sanchis, P. Modelling of PEM Fuel Cell Performance: Steady-State and Dynamic Experimental Validation. *Energies* **2014**, *7*, 670–700. [CrossRef]
20. Pérez-Page, M.; Pérez-Herranz, V. Effect of the Operation and Humidification Temperatures on the Performance of a Pem Fuel Cell Stack on Dead-End Mode. *Int. J. Electrochem. Sci.* **2011**, *6*, 492–505.

21. Derbeli, M.; Barambones, O.; Ramos-Hernanz, J.A.; Sbita, L. Real-Time Implementation of a Super Twisting Algorithm for PEM Fuel Cell Power System. *Energies* **2019**, *12*, 1594. [CrossRef]
22. Restrepo, C.; Konjedic, T.; Garces, A.; Calvente, J.; Giral, R. Identification of a Proton-Exchange Membrane Fuel Cell's Model Parameters by Means of an Evolution Strategy. *IEEE Trans. Ind. Inform.* **2015**, *11*, 548–559. [CrossRef]
23. Zhao, J.; Jian, Q.; Luo, L.; Huang, B.; Cao, S.; Huang, Z. Dynamic behavior study on voltage and temperature of proton exchange membrane fuel cells. *Appl. Therm. Eng.* **2018**, *145*, 343–351. [CrossRef]
24. Ma, T.; Lin, W.; Yang, Y.; Cong, M.; Yu, Z.; Zhou, Q. Research on Control Algorithm of Proton Exchange Membrane Fuel Cell Cooling System. *Energies* **2019**, *12*, 3692. [CrossRef]
25. Benziger, J.; Chia, E.; Moxley, J.; Kevrekidis, I. The dynamic response of PEM fuel cells to changes in load. *Chem. Eng. Sci.* **2005**, *60*, 1743–1759. [CrossRef]
26. Wu, J.; Yuan, X.; Martin, J.; Wang, H.; Zhang, J.; Shen, J.; Wu, S.; Merida, W. A review of PEM fuel cell durability: Degradation mechanisms and mitigation strategies. *J. Power Sources* **2008**, *184*, 104–119. [CrossRef]
27. Schmittinger, W.; Vahidi, A. A review of the main parameters influencing long-term performance and durability of PEM fuel cells. *J. Power Sources* **2008**, *180*, 1–14. [CrossRef]
28. Panha, K.; Fowler, M.; Yuan, X.; Wang, H. Accelerated durability testing via reactants relative humidity cycling on PEM fuel cells. *Appl. Energy* **2012**, *93*, 90–97. [CrossRef]
29. Zhang, D. *Contribution to Prognostics of PEM Fuel Cells: Approaches Based on Degradation Information at Multiple Levels*; Communauté Université Grenoble Alpes: Grenoble, France, 2018.
30. Gemmen, R.; Johnson, C. Evaluation of fuel cell system efficiency and degradation at development and during commercialization. *J. Power Sources* **2006**, *159*, 646–655. [CrossRef]